Rate Coefficient for the Reaction: $O + NO_2 + M \rightarrow NO_3 + M$

James B. Burkholder* and A. R. Ravishankara†

Aeronomy Laboratory, National Oceanic and Atmospheric Administration, 325 Broadway, Boulder, Colorado 80303

Received: January 12, 2000; In Final Form: May 22, 2000

The rate coefficient for the reaction $O(^3P) + NO_2 + M \rightarrow NO_3 + M$ (M = N_2), k_{1b}, was measured over the pressure range 20−800 Torr (N_2) between 220 and 296 K. Pulsed laser photolysis of NO_2 at 352 nm was used to produce O atoms and transient long-path diode laser absorption at 662 nm was used to detect NO_3 produced in the reaction. The pressure and temperature dependence of the measured rate coefficient is reproduced by the expression $k_{1b}(T,M) = [k_0(T)[M]/(1 + (k_0(T)[M]/k_\infty(T))]F_c^x$, where $x = \{1 + [\log(k_0(T)[M]/k_\infty(T))]^2\}^{-1}$ and $k_0(T) = k_0(300)\ (T/300)^{-n}$, $k_\infty(T) = k_\infty(300)\ (T/300)^{-m}$ with $k_0 = 3 \times 10^{-31}$ cm^6 molecule^{-2} s^{-1}, $n = 1.75$, $k_\infty = 3.75 \times 10^{-11}$ cm^3 molecule^{-1} s^{-1}, $m = 0$, and $F_c = 0.6$. This fit does not yield unique values for k_∞ or k_0 but are presented here merely to obtain $k_{1b}(T,M)$ for atmospheric modeling purposes. The reported values are significantly larger than the current recommendation for stratospheric modeling. Our larger values do not significantly increase the role of the title reaction in the Earth's atmosphere in terms of either ozone loss rate or conversion of reactive nitrogen oxides to less reactive forms such as HNO_3.

Introduction

NOx species, NO and NO_2, play critical roles in atmospheric ozone chemistry: they lead to photochemical ozone production in the troposphere and the lower stratosphere and catalytic ozone destruction in a large portion of the stratosphere. In the stratosphere, the reactions of NOx species affect both the ozone abundance and its vertical profile. The ozone destruction cycle

$$O(^3P) + NO_2 \rightarrow O_2 + NO \quad (1a)$$

$$O_3 + NO \rightarrow O_2 + NO_2 \quad (2)$$

$$\text{net:} \quad O(^3P) + O_3 \rightarrow 2O_2 \quad (3)$$

is the most important NO_x catalyzed cycle in the stratosphere. Reaction 1a has been studied many times in the past and we have recently revised the rate coefficient for this reaction.[1] However, there is only limited data available for the termolecular reaction of $O(^3P)$ addition to NO_2.[2−4]

$$O(^3P) + NO_2 + M \rightarrow NO_3 + M \quad (1b)$$

This reaction has been recognized for a long time,[2] and its rate coefficient has been estimated in various studies. Of these earlier studies, the works of Johnston[3] and Troe[4] and their colleagues are most quantitative. In none of the studies was the reaction isolated to extract the rate coefficient. It is, of course, impossible to separate (1b) from (1a), since they occur together and they may even be the same reaction leading to two sets of products.

Harker and Johnston[3] measured the formation of N_2O_5 in the continuous wave (cw) photolysis of NO_2. By fitting the measured NO_2 and N_2O_5 temporal profiles, they determined k_{1b} to be 8.2×10^{-32} cm^6 molecule^{-2} s^{-1} at 298 K in 1 atm of nitrogen. Hippler et al.[4] (for previous studies from this group, see references within) studied the pressure dependence of reaction 1b at 298 K for a variety of bath gases. They also employed cw photolysis of NO_2 and monitored the time dependence of the NO_2 loss. The values of k_{1b} from these two studies are in reasonable agreement. On the basis of these works, it is believed that the termolecular channel is a minor process for the loss of NO_2 or the formation of NO_3 under stratospheric conditions. To our knowledge, the temperature dependence of k_{1b} has not been previously reported.

In this work, we have obtained a more direct measure of k_{1b} and its temperature dependence. We photolyzed NO_2 at 352 nm (XeF excimer laser) to produce $O(^3P)$ and monitored the temporal profile of the NO_3 concentration via tunable diode laser absorption. The measured NO_3 absorption profiles can be analyzed to obtain k_1, $k_{1a} + k_{1b}$, and the measured concentration of NO_3 generated by this reaction can be used to obtain the branching ratio, k_{1b}/k_1. Our measured rate coefficients are compared with those of Hippler et al.,[4] which are currently recommended for atmospheric modeling.[5] The differences between the results of these two studies are discussed in relation to the impact of k_{1b} on atmospheric chemistry and ozone destruction cycles.

Experimental Details

The rate coefficient $k_{1b}(T,M)$ was measured by producing a known concentration of $O(^3P)$, henceforth referred to as O atoms, in an excess of NO_2, and then measuring the temporal profile of the absolute concentration of NO_3. The time constant for the formation of NO_3 is equal to the first-order rate coefficient for the loss of O atoms, which has contributions from both reactions 1a and 1b. To alter the competition for the consumption of O atoms between the fast bimolecular reaction (k_{1a}) and the minor termolecular channel (k_{1b}), NO_3 profiles were measured over a range of pressures and temperatures. O atoms were produced by pulsed laser (352 nm) photolysis of NO_2 in an excess of N_2, $(0.5−30) \times 10^{18}$ molecules cm^{-3}, at temperatures between 220 and 296 K. The temporal evolution of the

* Corresponding author. E-mail: Burk@al.noaa.gov.
† Also associated with Department of Chemistry and Biochemistry, University of Colorado, Boulder, CO 80309.

10.1021/jp000169z
Published on Web 07/01/2000

NO_3 product was monitored via diode laser absorption at 662 nm. The initial O atom concentration, $[O]_0$, was calculated from the photolysis laser fluence and the measured NO_2 concentration. The photolysis laser fluence was determined by photolyzing a known concentration of N_2O_5 and measuring the concentration of NO_3 produced. This actinometry was carried out using exactly the same experimental configurations as in the kinetic measurements by merely substituting N_2O_5 for NO_2 (see below). Details of the laser photolysis-time-resolved absorption apparatus and laser fluence calibration are described in Yokelson et al.[6] An outline of the apparatus and details specific to the current measurements are given below.

The apparatus consisted of (1) a reaction/absorption cell that was jacketed for temperature regulation and had an optical path length of 91 cm (single pass), (2) a diode array spectrometer, (3) a pulsed XeF (352 nm) excimer laser for photolysis, (4) a tunable visible diode laser (662 nm), and (5) a photodiode detector for measuring the intensity of the diode laser beam passing through the reactor. The glass cell (30 mm i.d.) was temperature controlled by circulating methanol from a temperature-regulated bath through its jacket. The temperature over the length of the absorption cell was constant to ±1 K. The concentrations of N_2O_5 and NO_2 were measured in the reactor with a D_2 lamp and a 0.5 m spectrograph equipped with a diode array detector. Absorption spectra between 200 and 365 nm were recorded, and the concentrations were quantified using the entire spectrum by using literature absorption cross sections.[1,5]

The photolysis and probe laser beams copropagated the length of the reactor. The photolysis laser beam filled the diameter of the cell, while the diode laser beam (2×3 mm) passed through the center of the cell. Measurements made by passing the diode laser beam off the center line of the reactor also yielded the same results. Either the diode laser or the D_2 lamp beam, but not both, passed through the absorption cell at a given time.

The diode laser ran single mode with an output power between 0.5 and 2 mW at 662 nm. The laser wavelength was locked to the peak of the NO_3 absorption feature at 661.9 nm by regulating the laser current (~40 mA) and temperature (~ 275 K). The NO_3 absorption cross sections and its temperature dependence were taken from Yokelson et al.[7] The detection limit for NO_3 in this system was $\sim 2 \times 10^{10}$ molecules cm^{-3} for a single photolysis laser shot.

O atoms were generated by 352 nm (XeF excimer laser) photolysis of NO_2.

$$NO_2 + h\nu \rightarrow NO + O \qquad (4)$$

The O atoms were consumed almost exclusively through reaction 1. The laser fluence and $[NO_2]_0$ were varied such that $[O]_0$ was $(1-6) \times 10^{12}$ atoms cm^{-3}.

A stable flow of NO_2 in N_2 was established through the reaction cell. The NO_2 concentration was measured using the diode array spectrometer. The intensity of the diode laser beam was monitored for ~1 ms before the photolysis laser was fired. The temporal profile of the 662 nm beam intensity was monitored for 4−9 ms after the laser pulse. Depending on the signal strength, profiles from 10 and 50 laser shots (0.1 Hz repetition rate) were coadded to improve the measurement signal-to-noise ratio. Using the intensity of the diode laser before the excimer pulse as I_0, the postphotolysis NO_3 absorbance was calculated. Thus, we measured the changes in NO_3 concentration. The NO_2 concentration was then remeasured to confirm its stability during the measurements of NO_3 temporal profiles. This sequence was repeated three to six times with different initial NO_2 concentrations (constant photolysis laser fluence) at each temperature and pressure. The laser fluence was kept low enough to ensure that $[O]_0$ was very small compared to $[NO_2]$ such that O atoms obeyed pseudo-first-order kinetics. Each NO_3 absorption profile, measured at 220, 240, 260, and 296 K and over the number density range $(0.5-28) \times 10^{18}$ molecules cm^{-3} (N_2), was analyzed to obtain values for $k_{1b}(T,M)$.

Laser Fluence Calibration. Determination of k_{1b} from the measured $[NO_3]$ profile requires accurate determinations of $[O]_0$ and NO_3 product concentrations. The O atom concentration was obtained from the photolysis laser fluence and the initial NO_2 concentration. The photolysis laser fluence (LF) was calibrated for each set of kinetic measurements. In several cases, the laser fluence was determined both before and after the kinetic measurements and found to agree within 5%. Measurements at $T < 298$ K were preceded by room-temperature calibrations. N_2O_5 photolysis at 352 nm,

$$N_2O_5 + h\nu \rightarrow NO_2 + NO_3 \qquad (5)$$

with NO_3 detection, as described above, was used as the actinometer. The NO_3 quantum yield from reaction 5 at 352 nm has been measured to be unity (see Harwood et al.[8] and references therein). This approach enabled us to both calibrate the fluence and measure k_{1b} by detecting the same species, NO_3, and therefore greatly reduced possible systematic errors. Specifically, this method eliminated the errors in the absorption cross section of NO_3 at 662 nm at 298 K.

The excimer laser fluence (LF), photon cm^{-2}, was determined from the slopes of plots of measured $[NO_3]_0$ vs $[N_2O_5]$

$$LF = [NO_3]_0/([N_2O_5]\sigma(N_2O_5)) \qquad (6)$$

where $[NO_3]_0$ is the NO_3 concentration produced by the laser pulse and $\sigma(N_2O_5)$ is the N_2O_5 absorption cross section at the photolysis wavelength (352 nm), 1.90×10^{-21} cm^2 $molecule^{-1}$ at 296 K. The N_2O_5 concentration was determined using the spectrum measured by the diode array spectrometer. For each calibration, four to six different N_2O_5 concentrations in the range $(5-20) \times 10^{15}$ molecules cm^{-3} were used. The total pressure was ~100 Torr (N_2). NO_2 and NO_3 were unavoidably present in the N_2O_5 sample from the equilibrium reaction

$$NO_2 + NO_3 + M \leftrightarrow N_2O_5 + M \qquad (7)$$

NO_2 was quantitatively determined using the absorption spectrum used to obtain the N_2O_5 concentration. NO_3 was estimated from the change in diode laser signal before and during the flow of the N_2O_5 sample. The measured NO_2, NO_3, and N_2O_5 concentrations yielded an equilibrium constant for reaction 7, which agreed within 10% with the value reported in DeMore et al.[5] A small correction, <5%, to the NO_3 signal in eq 6 was made to account for NO_2 photolysis, reaction 4, followed by reaction 1b. The NO produced in reaction 4 ultimately reacted with the NO_3 produced in reaction 1b.

$$NO_3 + NO \rightarrow NO_2 + NO_2 \qquad (8)$$

During the course of these experiments the excimer laser fluence was varied by a factor of ~3 by changing the laser discharge voltage. The initial O atom concentration was calculated using

$$[O]_0 = [NO_2]\sigma(NO_2)\,LF\,\Phi_4 \qquad (9)$$

where $[NO_2]$ was determined from the measured diode array spectrum, $\sigma(NO_2)$ is the NO_2 cross section at the photolysis

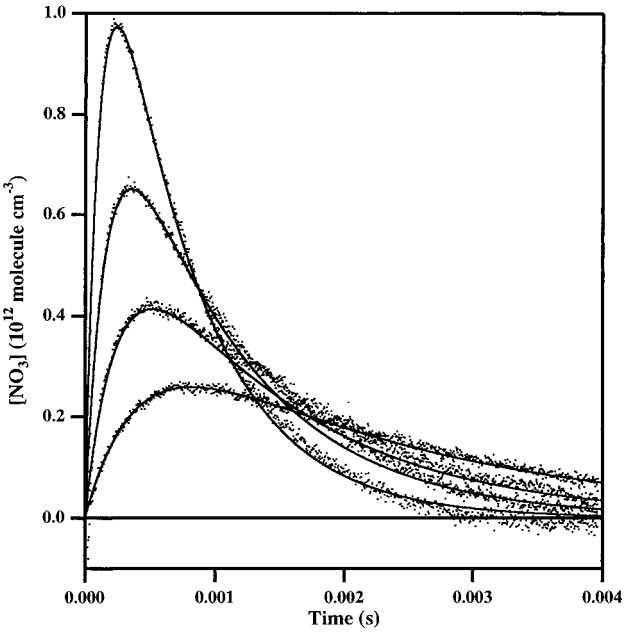

Figure 1. Representative NO_3 measurements following 352 nm photolysis of NO_2/N_2 mixtures at 296 K and 533 Torr total pressure. NO_2 concentrations were 6.60, 4.40, 2.92, and 1.97 $\times$ 10^{14} molecules cm^{-3}. The maximum NO_2 concentration corresponds to the profile with the largest peak NO_3 signal. The excimer laser fluence was 2.19 $\times$ 10^{16} photons cm^{-2}. The solid lines represent the best fit to the data (see text for details) with k_{1b} values of 2.70, 2.75, 2.70, and 2.60 $\times$ 10^{-12} cm^3 $molecule^{-1}$ s^{-1} and k_{12} values between 130 and 200 s^{-1}.

wavelength (352 nm) (determined from diode array spectra relative to the value at 413.4 nm[1]), LF is the laser fluence as determined above, and Φ_4 is the O atom quantum yield for reaction 4, which is taken to be unity. The NO_2 fractional photolysis varied from 0.006 to 0.017; thus, the $[NO_2]/[O]_0$ ratio was always greater than 59. The measured rate coefficients were found to be independent of the laser fluence and $[O]_0$ over this range.

Materials. NO_2 was prepared by reacting purified NO with excess O_2 that had been passed through a molecular sieve trap at dry ice temperature. NO_2 was collected in a dry ice cooled trap and purified by trap-to-trap distillation in an excess O_2 flow until a pure white solid remained. NO_2 was introduced into the gas flow from a mixture of 5% NO_2 in N_2 or O_2. N_2O_5 was prepared in a slow flow by reacting excess O_3, directly from a commercial ozonizer, with NO_2 at atmospheric pressure. The N_2O_5 was trapped and stored at 195 K. N_2O_5 was introduced into the reactor by passing a small N_2 flow through the trap. The temperature of the N_2O_5 trap was varied between 253 and 268 K during the calibration measurements. Purified HNO_3 was prepared by mixing reagent grade HNO_3 with concentrated H_2SO_4 in a 1:3 ratio. N_2 (UHP, >99.9995%) and He (UHP, >99.999%) were used as supplied. The linear flow velocities in the absorption cell were 6−15 cm s^{-1} such that the reactor was completely replenished with a fresh gas mixture between laser pulses.

Results and Discussion

Figure 1 shows a typical set of NO_3 temporal profiles measured following the 352 nm pulsed-laser photolysis of NO_2 at 296 K in 533 Torr of N_2. The NO_3 concentration reached a maximum value within the first millisecond followed by a decay almost back to the baseline within the next 5 ms. The peak NO_3 concentration, the time to reach the maximum, and the loss rate of NO_3 were all dependent on the initial NO_2 concentration. Therefore, the NO_3 production and loss processes could not be separated in time in this chemical system. k_{1b} could be obtained from an analysis of the pressure and temperature dependence of k_1 determined from NO_3 rise times, i.e., changes in k_1, and/or from the absolute NO_3 yield relative to the initial O atom concentration. The change in k_1 over the conditions used in this study ranges from ~5% at room temperature and low pressure to about 40% at 220 K and 800 Torr. Therefore, the determination of these relatively small changes in k_1 is less accurate than the absolute NO_3 concentration measurements. k_{1b} was obtained by simulating the measured NO_3 temporal profiles using the reaction mechanism outlined in Table 1 with the measured photolysis laser fluence and $[NO_2]_0$. k_{1a} is well-defined from previous studies[1] and therefore was fixed in the analysis. Therefore, k_{1b} was determined from analyzing NO_3 formation with a knowledge of $[O]_0$ and the absolute concentration of NO_3 formed. The first 25 μs of the measured NO_3 profiles were not used in the analysis because scattered light from the photolysis pulse influenced these data. However, the time of the photolysis pulse was well-defined.

TABLE 1: Reaction Mechanism

reaction		rate coefficient[a]	ref
$O + NO_2 \rightarrow O_2 + NO$	(1a)	$5.22 \times 10^{-12} \exp(210/T)$	1
$O + NO_2 + M \rightarrow NO_3 + M$	(1b)	determined in fit	
$O + NO_3 \rightarrow NO_2 + O_2$	(10)	1.0×10^{-11}	5
$O + NO + M \rightarrow NO_2 + M$	(11)	$k(T,M)$[b]	5
		$k_0 = 9.0 \times 10^{-32}$; $n = 1.5$	
		$k_\infty = 3.0 \times 10^{-11}$; $m = 0$	
$NO + NO_3 \rightarrow NO_2 + NO_2$	(7)	$1.5 \times 10^{-11} \exp(170/T)$	5
$NO_2 + NO_3 + M \rightarrow N_2O_5 + M$	(8)	$k(T,M)$	5
		$k_0 = 2.2 \times 10^{-30}$; $n = 3.9$	
		$k_\infty = 1.5 \times 10^{-12}$; $m = 0.7$	
$NO_3 \rightarrow$ loss	(12)	varied in fit	

[a] Units: first order reaction, s^{-1}; second order reactions, cm^3 $molecule^{-1}$ s^{-1}; third order reactions cm^6 $molecule^{-2}$ s^{-1} [b] $k_0(T) = k_0(300)\,(T/300)^{-n}$, $k_\infty(T) = k_\infty(300)\,(T/300)^{-m}$; $k(T,M) = [k_0(T)\,[M]/(1+(k_0(T)[M]/k_\infty(T))\,]0.6^x$; $x = \{1 + [\log(k_0(T)[M]/k_\infty(T))]^2\}^{-1}$.

The results of the simulations are shown in Figure 1 as the solid lines. Very good agreement between the measured and simulated data was achieved for all experimental conditions (i.e., temperature and pressure). For a set of NO_3 profile measurements at a given pressure and temperature, the fit was optimized by varying k_{1b} for each $[NO_2]$ used. The average of these values is then reported for $k_{1b}(T,M)$.

The data at longer times, >2 ms, shown in Figure 1 were best reproduced when an additional NO_3 first-order loss rate coefficient, k_{12}, of between 30 and 200 s^{-1} was included in the fit. This first-order loss rate coefficient showed a slight increase with increasing pressure and decreasing temperature. Reactions 7 and 8 represent the most significant loss processes for NO_3 in our experiments and account for NO_3 loss rate coefficients of 300−1000 s^{-1}, depending on $[NO_2]$. Increasing the values of k_8, by 10−40%, would have nearly the same affect in the fit as including k_{12}. We checked the value of k_7 under our experimental conditions by measuring the NO_3 decay following HNO_3 photolysis (248 nm)

$$HNO_3 + h\nu \rightarrow OH + NO_2 \qquad (13)$$

in the presence of NO_2. The OH radical produced in reaction 13 reacted with HNO_3

$$OH + HNO_3 \rightarrow H_2O + NO_3 \qquad (14)$$

to produce NO_3.[9] NO_3 loss was measured under pseudo-first-

TABLE 2: Summary of O + NO_2 + M Rate Coefficients

T (K)	[N_2] (10^{18} molecule cm^{-3})	k_{1b} (10^{-12} cm^3 $molecule^{-1}$ s^{-1})	*T* (K)	[N_2] (10^{18} molecule cm^{-3})	k_{1b} (10^{-12} cm^3 $molecule^{-1}$ s^{-1})
220	26.3	4.9	296	26.6	4.84
	17.6	4.0		8.05	2.22
	4.25	1.39		8.44	1.75
	30.8	9.14		9.06	2.22
	22.3	6.96		0.675	0.52
	12.9	5.2		24.78	3.97
	6.14	2.35		11.41	2.43
240	3.14	1.09		3.16	0.92
	9.93	2.98		6.39	1.35
	18.78	4.46		10.79	2.48
	28.2	6.62		17.38	2.69
	2.17	1.05		24.84	3.22
	21.5	4.55		3.26	1.05
	13.47	3.17		6.91	1.32
	17.16	4.06		11.15	2.62
	13.87	3.9		18.12	3.48
	6.63	1.42		24.03	4.35
260	14.7	3.61		16.5	3.38
	18.4	4.06		10.56	2.36
	22.8	4.65		6.259	1.34
	27.4	5.78		3.195	0.87
	3.71	1.0			
	12.0	3.57			

order conditions in NO_3 at 240 K (P = 390 Torr) and 296 K between 80 and 700 Torr. The values of k_7 determined from these mesurements are in reasonable agreement with those recommended in DeMore et al.,[5] with our measured values being systematically higher by ~10−15%. However, this 10−15% difference is not sufficient to completely account for the observed higher NO_3 loss rate. Reaction 8, which makes a smaller contribution to the NO_3 loss, has been extensively studied with good agreement in the rate coefficient and its temperature dependence.[5] This rate coefficient may be enhanced if NO was vibrationally excited. A small, ~1%, NO impurity in the NO_2 sample would also be sufficient to account for the observed larger loss rate coefficient. However, when an NO_2 sample was taken from a mixture of NO_2 in O_2 (which should convert NO to NO_2), the enhanced NO_3 loss was still observed. UV absorption measurements between 200 and 250 nm of the NO_2/O_2 mixture showed the NO impurity level to be less than ~0.5%. Therefore, a partial contribution from a NO impurity cannot be ruled out.

Although the source of the enhanced NO_3 loss (over those given in Table 1) is not clearly identified, including k_{12} in the fitting had less than a 5% effect on the derived value of k_{1b}. At a given temperature and pressure (different NO_2), the 1σ precision of the retrieved k_{1b} values was better than 10% of the mean. Our measured NO_3 profiles were not well fitted if k_{1a} was varied by more than 10% of the value shown in Table 1.

A summary of the $k_{1b}(T,M)$ values obtained over the temperature range 220−296 K are given in Table 2. Each $k_{1b}(T,M)$ value quoted in Table 2 represents the average of four to six individual determinations (similar to those shown in Figure 1). The rate coefficient data is also shown graphically in Figure 2.

The rate coefficient for reaction 1b is in its falloff region over the number density range covered in our measurements, Figure 2. Our measurements do not extend to high enough pressures to determine the high-pressure limit. We have fit our data to the expression used in the NASA and IUPAC evaluations for atmospheric modeling,[5,10]

$$k_{1b}(T,M) = [k_0(T)[M]/(1+ (k_0(T)[M]/k_\infty(T))]0.6^x \quad (15)$$

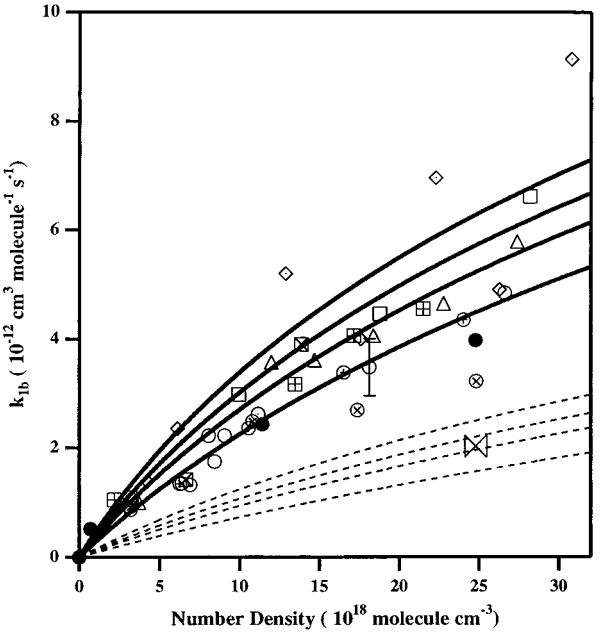

Figure 2. Rate coefficient data for O + NO_2 + M → NO_3 + M measured in this work at 220 (diamonds), 240 (squares), 260 (triangles), and 296 (circles) K. The symbol fill is different for measurements made in different sets. Solid lines are calculated using the parameters given in the text. The error bar shows a representative uncertainty (see text). Dashed lines are the values calculated using the parameters of Hippler et al.[4] at the same temperatures measured in this work. The value reported by Harker and Johnson[3] is also shown (large bow tie).

where $x = \{1 + [\log(k_0(T)[M]/k_\infty(T))]^2\}^{-1}$ and $k_0(T) = k_0(300)$ $(T/300)^{-n}$ and $k_\infty(T) = k_\infty(300)$ $(T/300)^{-m}$ (F_c = 0.6). Our data clearly show a systematic dependence on temperature, and the following values reproduce our rate coefficient data within the measurement precision:

$$k_0 = 3 \times 10^{-31}\ cm^6\ molecule^{-2}\ s^{-1};\ n = 1.75$$

$$k_\infty = 3.75 \times 10^{-11}\ cm^3\ molecule^{-1}\ s^{-1};\ m = 0$$

The data used to derive these parameters covers the pressures and temperatures found over most of the atmosphere. The precision of the measurements and the magnitude of the temperature dependence in k_{1b} do not allow for an accurate determination of the n parameter. Our fit does not yield unique values for k_∞ or k_0 but are presented here merely to obtain $k_{1b}(T,M)$ for atmospheric modeling purposes. A fit of our data using k_∞ given by Troe's group[4] does not reproduce our rate coefficients as well as the values given above. For comparison, in Figure 2 we have also shown the rate coefficients calculated using the parameters reported by Hippler et al.[4] and adopted by DeMore et al.[5] These rate coefficients are systematically lower than the present measurements by factors of between 2 and 4. Also, the temperature dependence is somewhat different from the recommendation that is based on analogy with similar termolecular reactions.

Again, we stress that we have not determined k_∞ from our data. This is because our highest pressure (800 Torr) measurements are not large enough to approach the high-pressure regime for this reaction. Furthermore, as described below, it is not clear if a unique high-pressure limiting rate coefficient can even be assigned to this reaction. Troe has examined this reaction extensively and noted that the intermediate formed in the O +

NO_2 reaction to be quenched to NO_3 may convert to an intermediate that yields $O_2 + NO$. We would like to point out that the same intermediate, NO_3*, may be involved in both reactions 1a and 1b. In this case, the high-pressure-limited rate coefficient would simply be the rate coefficient for the formation of the NO_3* intermediate. In other words, if reactions 1a and 1b are not separate competing reactions, the high-pressure-limiting rate constant will not be uniquely attributed to reaction 1b and using the simple formula for an association reaction would be inappropriate.

The accuracy of k_{1b} reported in this study depends on the accuracies of the photolysis laser fluence, NO_2 concentration, NO_2 absorption cross section at the photolysis wavelength, and the precision of the individual NO_3 profile measurement/analysis. However, we designed our experiments to minimize systematic errors. The accuracy of k_{1b} depends mostly on the uncertainties in the quantum yields for the formation of O atom from NO_2 (Φ_1) and NO_3 from N_2O_5 (Φ_2) photolyses and the relative temperature dependence in the absorption cross section of NO_3 at 662 nm. We estimate the uncertainties in the fit of the data to the measured profiles to be ~10% at 296, 260, and 240 K and ~20% at 220 K. The quantum yields Φ_1 and Φ_2 are estimated to be uncertain by 5 and 15%, at the 95% confidence levels. The relative temperature dependence of the NO_3 absorption cross section is estimated to be at most 15% at the 95% confidence level. On the basis of these uncertainties, we estimate the accuracy of the k_{1b} values to be ±15% (67% confidence limits) at 296, 260, and 240 K and ~20% at 220 K, while the measured pressure and temperature dependencies are expected to be more accurate.

Hippler et al. determined k_{1b} by modeling their measured NO_2 quantum yield following cw 366 nm photolysis of NO_2 in various bath gases. Although it is not possible to evaluate their data quantitatively, the differences in k_{1b} may be due to the sensitively of the modeling analysis to secondary chemistry such as reactions 7 and 8. The rate coefficients for these reactions have been revised substantially since the study of Hippler et al. For example, both k_7 and the equilibrium constant for reaction 8 have been increased by a factor of 3 in studies carried out after Hippler et al.'s study. Also, we now know that N_2O_5 could be hydrolyzed on the walls of the reactor, if water is present. It should be noted that the experiments of Troe's group were designed to be nearly independent of k_7 and k_8, but in reality they had to account for these reactions.

Atmospheric Implications. The reaction of O atoms with NO_2 can affect the loss rate of odd oxygen (O and O_3) and alter the rate of conversion of NO_2 to species such as N_2O_5 and HNO_3 that are longer lived and less reactive in the stratosphere. Here, we will very briefly examine the impact of the nearly a factor of 2 larger value of k_{1b} measured here relative to those used in current stratospheric calculations. These calculations do not represent a comprehensive modeling study. However, we can show the impact of the revised rate coefficient for a typical condition and qualitatively extrapolate to global conditions.

The calculated rate of conversion of NO_2 to N_2O_5 and, subsequently to HNO_3 via heterogeneous hydrolysis on sulfate aerosol or polar stratospheric clouds, is not affected by our higher value of k_{1b}. This is because NO_3 produced in the reaction is very rapidly (within a few seconds) photolyzed and does not allow for the production of N_2O_5 via the reaction of NO_3 with NO_2.

On the other hand, the conversion of NO_2 to NO_3 via reaction 1b may enhance the NOx catalyzed ozone destruction rate. To evaluate this possibility, we compare the rates of the rate-limiting steps in the involved catalytic ozone destruction cycles.

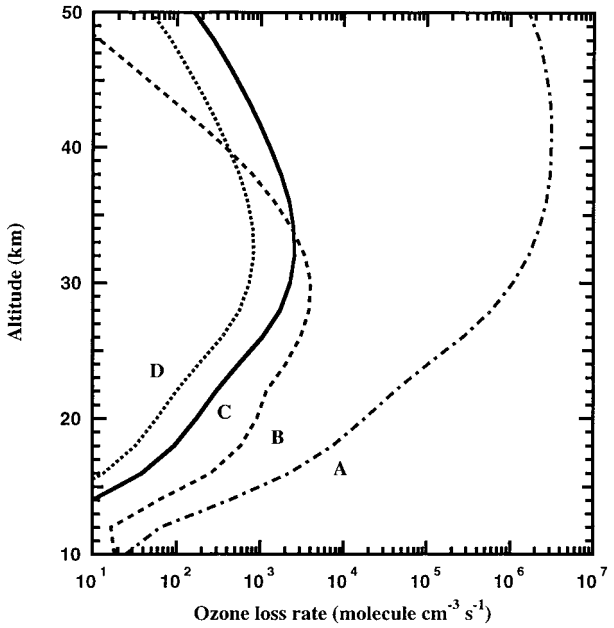

Figure 3. Rate of ozone loss rate due to the catalytic cycles discussed in the text plotted as a function of altitude in the stratosphere. The concentrations of O, O_3, NO, and NO_2 as well as the temperature and number density were taken from a 2-D model of Solomon and Garcia.[11] Line A is for reaction 1a, B is for reaction 17, C is for reaction 1b with our values of the rate coefficient, and D is for reaction 1b with the value of k_{1b} recommended by DeMore et al.[5]

$$NO + O_3 \rightarrow NO_2 + O_2 \quad (2)$$

$$O + NO_2 \rightarrow NO + O_2 \quad (1a)$$

$$\text{net:} \quad O + O_3 \rightarrow 2O_2 \quad (3)$$

$$NO + O_3 \rightarrow NO_2 + O_2 \quad (2)$$

$$O + NO_2 + M \rightarrow NO_3 + M \quad (1b)$$

$$NO_3 + h\nu \rightarrow NO + O_2 \quad (16)$$

$$\text{net:} \quad O + O_3 \rightarrow 2O_2 \quad (3)$$

$$NO + O_3 \rightarrow NO_2 + O_2 \quad (2)$$

$$NO_2 + O_3 \rightarrow NO_3 + O_2 \quad (17)$$

$$NO_3 + h\nu \rightarrow NO + O_2 \quad (16)$$

$$\text{net:} \quad 2O_3 \rightarrow 3O_2 \quad (18)$$

The reaction scheme where NO_3 (produced via (1b) or (17)) is photolyzed to NO_2 and O does not lead to a net loss of odd oxygen, and hence, it is not included here. The rates (i.e., the products of the rate coefficients and the concentrations of the species involved in the reactions) of the rate-limiting steps in these three cycles, reactions 1a, 1b, and 17, are plotted in Figure 3, for 40°N for a solar zenith angle of 45°. The branching ratio for production of NO and O_2 in NO_3 photolysis as well as all the necessary rate coefficients (other than k_{1a} and k_{1b}) are from DeMore et al.[5] The value of k_{1a} is from Gierczak et al.[1] The rates of these reactions will be similar for other solar zenith angles (i.e., <~85°), locations, and seasons since only visible radiation is involved in the photolysis reactions and it is not attenuated greatly with the solar zenith angle. Also, the small temperature changes with season will not lead to large changes

in the calculated rates of these processes. For the case of reaction 1b, we show rates calculated using the rate coefficients reported here and the recommended values. It is clear that the rate of ozone loss due to reaction 1a (i.e., the reaction of O with NO_2 to give NO and O_2) is much greater than that due to the other cycles. At lower altitudes, the rates of ozone destruction due to the formation of NO_3 become a significant (5−10%) fraction of the ozone destruction by NO_x. Here, the contribution of the revised value of k_{1b} to the NO_x-catalyzed ozone loss is small, but not negligible. However, at the lower altitudes (i.e., $<\sim$25 km), stratospheric ozone loss is primarily controlled by odd-hydrogen-catalyzed ozone destruction,[12] and hence, the role of NO_x is greatly suppressed. Therefore, we conclude that the increase in k_{1b} by a factor of 2 over the currently recommended values will not have a significant effect on either the calculated natural ozone levels or the changes in ozone due to anthropogenic NO_x perturbations.

Acknowledgment. We thank R. Portmann for the atmospheric concentration profiles used in this paper. This work was funded in part by the upper atmospheric research program of NASA.

References and Notes

(1) Gierczak, T.; Burkholder, J. B.; Ravishankara, A. R. *J. Phys. Chem. A* **1999**, *103*, 877.
(2) Ford, H. W.; Endow, E. *J. Chem. Phys.* **1957**, *27*, 1156.
(3) Harker, A. B.; Johnston, H. S. *J. Phys. Chem*. **1973**, *77*, 1153.
(4) Hippler, H.; Schippert, C.; Troe, J. *Int. J. Chem. Kinet.*, Symposium No. 1, 1975, 27−38.
(5) DeMore, W. B.; Sander, S. P.; Golden, D. M.; Hampson, R. F.; Kurylo, M. J.; Howard, C. J.; Ravishankara, A. R.; Kolb, C. E.; Molina, M. J. Chemical Kinetics and Photochemical Data for Use in Stratospheric Modeling. Evaluation No. 11, JPL Publication 97-4; Jet Propulsion Laboratory: Pasadena, CA, 1997.
(6) Yokelson, R. J.; Burkholder, J. B.; Fox, R. W.; Ravishankara, A. R. *J. Phys. Chem. A* **1997**, *101*, 6667.
(7) Yokelson, R. J.; Burkholder, J. B.; Fox, R. W.; Talukdar, R. K.; Ravishankara, A. R. *J. Phys. Chem*. **1994**, *98*, 13144.
(8) Harwood, M. H.; Burkholder, J. B.; Ravishankara, A. R. *J. Phys. Chem. A* **1998**, *102*, 1309.
(9) Brown, S. S.; Burkholder, J. B.; Talukdar, R. K.; Ravishankara, A. R. Manuscript in preparation.
(10) Atkinson, R.; Baulch, D. L.; Cox, R. A.; Hampson, R. F.; Kerr, J. A.; Rossi, M. J.; Troe, J. *J. Phys. Chem. Ref. Data* **1999**, *28*, 191.
(11) Portmann, R. W.; Brown, S. S.; Gierczak, T.; Talukdar, R. K.; Burkholder, J. B.; Ravishankara, A. R. *Geophys. Res. Lett*. **1999**, *26*, 2387.
(12) WMO (World Meterorological Organization), Scientific Assessment of Ozone Depletion: 1998 (Global Ozone Research and Monitoring Progject Report No. 44, WMO, Geneva, 1999).